Preparation of a Library of EDTA Amide *x*-Aminenaphthalene-*y*-sulfonic Acid Derivatives on Solid Phase and Their Fluorescence Behavior toward Transition Metals

Hisila Santacruz Ortega,[†,‡] Georgina Pina-Luis,[‡] Sara Karime López,[‡] and Ignacio A. Rivero*[,‡]

Departamento de Investigación en Polímeros y Materiales, Universidad de Sonora, Apartado Postal 130, Hermosillo, 83000 Sonora, México, and Centro de Graduados e Investigación, Instituto Tecnológico de Tijuana, Apartado Postal 1166, Tijuana, 22000 B. C., México

Received May 11, 2009

In this work, we report the synthesis of a combinatorial library of 80 derivatives of EDTA amide *x*-aminenaphthalene-*y*-sulfonic acid on four different supports with variable length linker. The sensing fluorescence behavior of these materials for transitions metals was studied by packing the beads into a conventional flow-through cell in a continuous flow injection set up. The fluorescence emission response of these materials shows that sensors supported in Argopore (***a***) with the fluorescence moiety of 1-aminenaphthalene-4-sulfonic acid behaves like dosimeter for copper.

Introduction

The synthesis of sensor materials for the recognition, detection and measurement of different metal ions is of great importance in chemistry and biology. In particular, there is a growing interest in the synthesis of molecules capable of sensing and report the presence of transition and heavy metal ions. Molecules that can report the presence of metal ions through changes in optical properties provide a particularly convenient way of detecting a sensing event. Possibly, the most useful transduction scheme of this kind of systems is based either on the quenching or the enhancement of fluorescence.[1–7]

During the last years, the importance of separation and concentration techniques involving the immobilization of a reactive motif for the trace analysis has risen substantially.[8–11] The use of sorbent materials can provide a concentration factor up to several hundred fold, better separation of interfering ions, high efficiency and rate of the process, and the possibility of combining with different analytical techniques. In fact, several types of chelating resins have been developed by loading chelating ligands on a polymer matrix through both ion-exchange and hydrophobic interactions. Although these sorbent materials may exhibit good capacity they have low stability. Therefore, covalent linking of the ligand furnishes the basis for the development of selective and stable metal ion sorbents. Because of their high selectivity, chelating resins have been widely used as sorbent materials for metal ions.[12–15] Despite the fact that there are various chelating groups,[16–20] those derived of EDTA have high affinities toward metal ions.[21–25]

Because the conventional search in the design and discovery of novel sensing materials with the adequate transduction and recognition properties is considerably time-consuming, there is a strong need for the use of effective methods to increase the number of sensors that can be obtained each time. Combinatorial chemistry and solid phase synthesis have become a rational approach to make the discovery of new sensing materials more efficient and have been widely used in the generation and optimization of molecules with sensing and sorbent purposes.[26–29]

With this in mind, we now report the synthesis of a combinatorial library of EDTA amide as a receptor moiety on four different supports with variable length linker and naphthalene sulfonic derivatives as fluorescent motif. By exploiting the metal binding properties of EDTA, we combine the advantageous aspects of both fluorosensing with selective metal immobilization. The design of a metal ion fluorescent sensing sorbent consists of three components: (a) the metal ion recognition/retention moiety, (b) the optical reporter, and (c) the solid support. Screening of the library members for Cu^{2+}, Zn^{2+}, Ni^{2+}, Hg^{2+}, and Pb^{2+} binding response as sensing material was performed using fluorescence spectral changes, and their sorption capacity was evaluated. The role of the fluorescent motif, length linker and solid support is outlined.

Results and Discussion

The synthesis of immobilized EDTA amide *x*-aminenaphthalene-*y*-sulfonic acid (ANS) on four different supports was achieved by the route outlined in Scheme 1. Four representative resins, Argopore (***a***), Merrifield (4% DVB) (***b***), Merrifield (1% DVB) (***c***), and Wang (***d***), were used in this work. The latter was chlorinated with BTC/PPh_3P,[26] to obtain the corresponding chlorinated resin. The synthesis began with

* To whom correspondence should be addressed. E-mail: irivero@tectijuana.mx.
[†] Universidad de Sonora.
[‡] Instituto Tecnológico de Tijuana.

10.1021/cc900075r CCC: $40.75
Published on Web 10/12/2009

Scheme 1. General Method for the Synthesis of the Library of EDTA Amide *x*-Aminenaphthalene-*y*-sulfonic Acid Derivatives Supported on Resins

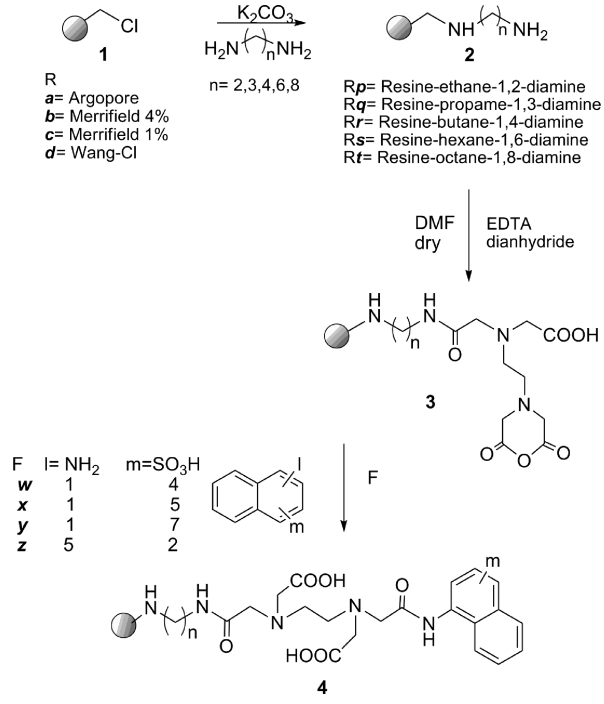

the attachment of the corresponding alkyl diamines, ethane-1,2-diamine (***p***), propane-1,3-diamine (***q***), butane-1,4-diamine (***r***), hexane-1,6-diamine (***s***), and octane-1,8-diamine (***t***), to the resin using the methodology reported by us in previous work,[27] to obtain the derivatives ***2***(***a***−***d***)(***p***−***t***) (Scheme 1). The next step involves the reaction with EDTA dianhydride in DMF to obtain resin derivatives ***3***(***a***−***d***)(***p***−***t***)**.** The resultant resins ***3*** were finally treated with the corresponding amine drivatives of NSA, 1-naphthylamine-4-sulfonic acid (***w***), 1-naphthylamine-5-sulfonic acid (***x***), 1-naphthylamine-7-sulfonic acid (***y***), and 5-naphthylamine-2-sulfonic acid (***z***), to obtain the resin products ***4***(***a***−***d***)(***p***−***t***)(***w***−***z***).

The various reaction steps were monitored by IR and fluorescence spectroscopy. In addition, to get the mass spectra data, the resins were treated with TFA/CH_2Cl_2 (1:1) for 30 min under ultrasonic conditions. The resins were filtered and 1 μL of the washing solution was directly injected on an ESI-MS for analysis. The corresponding molecular ions $[M + H]^+$ were obtained.

The design shown in Figure 1, represent a library of 4 × 5 × 4 EDTA bead products with diversity achieved by varying the solid support, spacer linker between resin and EDTA, and fluorescent motif.

Fluorimetric Characterization. Constant monitoring of the various synthesis steps was carried out by measuring on-bead fluorescence. Resins were transferred to a conventional flow-through fluorescence cell, and spectra were obtained directly from the dry resin beads. Fluorescence spectral data for all resins in this step are summarized in Table 1. The presence of the alkyldiamine led to a red shift in the emission spectra and increases the fluorescence emission, indicating that the resins were modified. On the other hand, the Kaiser test was positive for the presence of amino groups.

The fluorescence spectra of the final products obtained for all the resins with space linker ***r*** are shown in Figure 2 (***a***−***d***)***r***(***w***−***z***). The remaining library showed a similar spectral luminescence pattern. In fact, the excitation bands of the products show new bands in the 390−416 nm region, which are present in the UV−vis spectra obtained by diffuse reflectance. This behavior indicates the presence of the fluorescence moieties in the resins. Also, in the IR spectra of the final products, new bands of amide, sulfonic acid, and naphthalene are present, which supports the results obtained in fluorimetric characterization.

As can be seen, incorporation of EDTA amide *x*-aminenaphthalene-*y*-sulfonic acid derivatives into the resins is evidenced by a drastic decrease in the spectral characteristics. New bands at 395 and 410 nm in the excitation spectra, indicate the presence of *x*-amidenaphthalene-*y*-sulfonic acid on the solid support. The position of the sulfonic acid group substituent on the naphthalene unit proved to be important in the ability to quench naphthalene fluorescence. In general, the fluorescence motif with better properties was 1-amide-napthalene-4-sulfonic acid (***w***), whereas the worse emission properties were displayed by 1-amidenapthalene-7-sulfonic acid (***y***). The behavior of the library, using the fluorescence of the respective resin modified with corresponding diamine **2**(***a***−***d***)(***p***−***t***) as reference, is shown in S1 of Supported Information. Quenching of fluorescence emission can be attributed to several cooperative interactions between amide links to EDTA and naphthalenesulfonic acid. Reports by Wiczk et al.[28] suggest that the fluorescence quenching of the aromatic group occurs by photoinduced electron transfer process (PET) between the excited aromatic chromophore as a donor, and the electrophilic unit of carbonyl of amide group as an acceptor; the quenching efficiency is dependent on the distance between the aromatic and the amide group. An assumption that the PET process is responsible for the aromatic fluorescence quenching by the amide group means that the electron transfer rate constant should depend on the ionization potential of the excited chromophore (electron donor). The results in our work demonstrate that the position of the sulfonic acid group in the naphthalene amide has an important role in the PET process, in agreement to reports by Chernilevskaya.[29]

In addition, the lower emission of the materials supported on Merrifield (1% DVB) resin ***c*** can be attributed to a lower degree of cross-linking in this resin, which increases the interactions with the surrounding, thus allowing nonradiative deactivation of the fluorophores.

At this stage and taking into account the above results, we selected **4**(***a***−***d***)(***p***−***t***)(***w***,***z***) to check effect of water at different pH. Two excitation wavelengths were used, 466 nm for the resin, and 410 nm for the fluorescent moiety. Comparing the emission of the resin and the fluorescence motif in dry medium and wet medium, we found a 50% increase in the emission of resins and a >300% increase in the emission of ***w***. The emission intensity was virtually constant in the pH range studied (2−11). This behavior may be explained by the effect of solvation by water, which reduces the interactions and collisions between neighboring molecules, as well as the PET process between the chro-

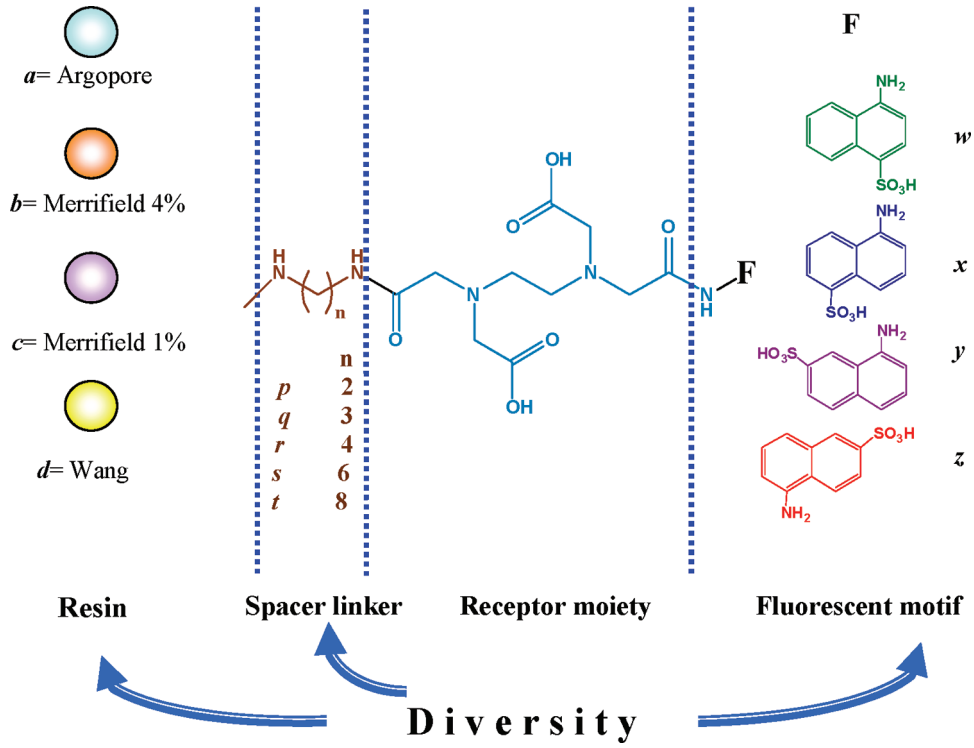

Figure 1. Fluorescent chemosensor library for metal ions.

Table 1. Fluorescence Spectra Data, Excitation Wavelength (λ_{ex}), Emission Wavelength (λ_{em}), and Relative Intensity of Argopore (***a***), Merrifield 4% DVB (***b***), Merrifield 1% DVB (***c***), and Wang (***d***) Resins and the Alkyldiamines Supported on Resins (***a*−*d*)(*p*−*t*)**

spacer linker			**p** $n = 2$			**q** $n = 3$			**r** $n = 4$			**s** $n = 6$			**t** $n = 8$		
resin	λ_{ex} nm	λ_{em} nm	λ_{ex} nm	λ_{em} nm	I/I_R	λ_{ex} nm	λ_{em} nm	I/I_R	λ_{ex} nm	λ_{em} nm	I/I_R	λ_{ex} nm	λ_{em} nm	I/I_R	λ_{ex} nm	λ_{em} nm	I/I_R
a	467	518	467	519	1.14	467	526	1.12	467	526	1.04	467	528	0.84	467	527	1.30
b	379	454	371	453	1.51	374	454	1.64	377	454	1.21	368	451	0.76	396	468	1.29
c	372	449	366	444	0.90	363	448	1.12	371	450	0.84	371	446	1.57	378	450	1.72
d	375	435	370	441	1.40	380	443	1.35	374	440	1.29	372	445	1.24	395	459	1.26

mophore and the amide group. The remaining library showed a similar behavior. The change in the fluorescence intensity of dry resin beads of ***apw*,** before and after passing water through fluorescence cell is shown in Supporting Information S2.

Metal Ion Recognition Properties of the Library with the Fluorescence Motif *w*. Evaluation of the materials with fluorescence motif ***w*** toward divalent transition metals ions Cu^{2+}, Ni^{2+}, Zn^{2+}, and Hg^{2+} and for the heavy metal Pb^{2+}, were achieved by packing the corresponding beads into conventional flow-through fluorescence cell and then pass the metal ion solutions using a continuous flow injection setup. Figure 3 shows the fluorescence spectra of the resin materials ***4*(*a*−*d*)(*r*)(*w*)**. Resin beads showed different behavior toward the evaluated metals, indicating a strong effect of the resin character in the fluorescence emission of sensor materials. The fluorescence motif ***w*** on resins ***b*** and ***c*** (Merrifield's with different cross-linking degree) showed similar behavior. Fluorescence responses were not appreciated in both cases when interaction with the metals takes place. In contrast, the same materials on resins ***a*** and ***d*** showed good properties like sensors because the fluorescence of ***w*** change in the presence of the metals. The linker group of the polymer resins Argopore (***a***) and Wang (***d***) are longer than Merrifield's (***b***,***c***), this difference in the structure of the resins might have an effect on the ability of the reactive sites to interact with the metals. In addition the degree of cross-linking greatly affects not only the ability of reactive sites to interact (loading, diffusion) but also the physical properties of the resin (e.g., swelling, rigidity).[30] Different fluorescence responses of the materials ***arw*** and ***drw***, may be attributed to the cross-linking degree. In resin ***a*** the cross-linking degree is higher than in ***d***, which gives a greater rigidity of the structure matrix and prevents expansion of the polymer backbone, discouraging response from the fluorescent material supported on resin ***a*** toward metals.[31]

The best properties as sensor were found in the materials supported on resin ***a***, since the changes in the fluorescence response with the metals studied were greater. In the case of ***rz*** supported on ***d***, the inability to discriminate between the two metals (Ni^{2+} and Cu^{2+}) suggests that the properties are not the most appropriate. For this reason we decided to select resin ***a*** for the following studies.

Figure 4 shows the change in the fluorescent properties of the selected library ***4*(*a*)(*p*−*t*)(*w*)** in the presence of the metals under study. In contrast with the metal ions Cu^{2+}, Ni^{2+}, and Zn^{2+}, the presence of heavy metal ions Hg^{2+} and Pb^{2+} did not indicate changes in the emission of the unit

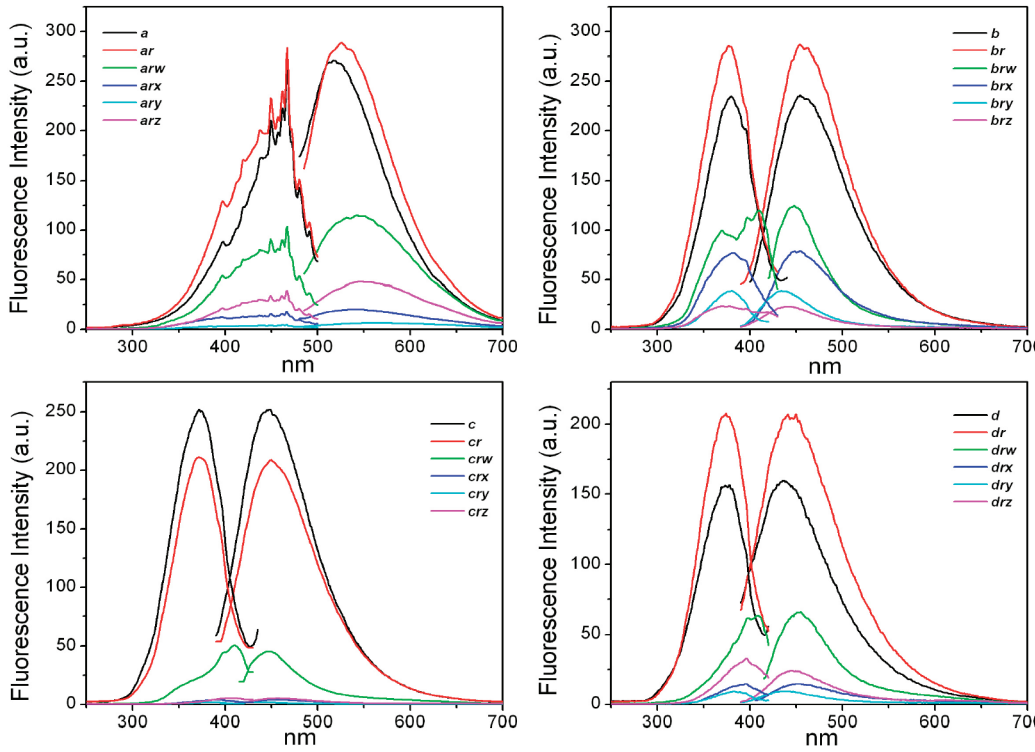

Figure 2. Fluorescence spectra of dry resins. The upper line of the insert on each spectrum indicates the kind of resin (***a*−*d***), spacer linker (***r***) supported on resins (***a*−*b*)*r***, and final products (***a*−*d*)*r*(*w*−*z*)**.

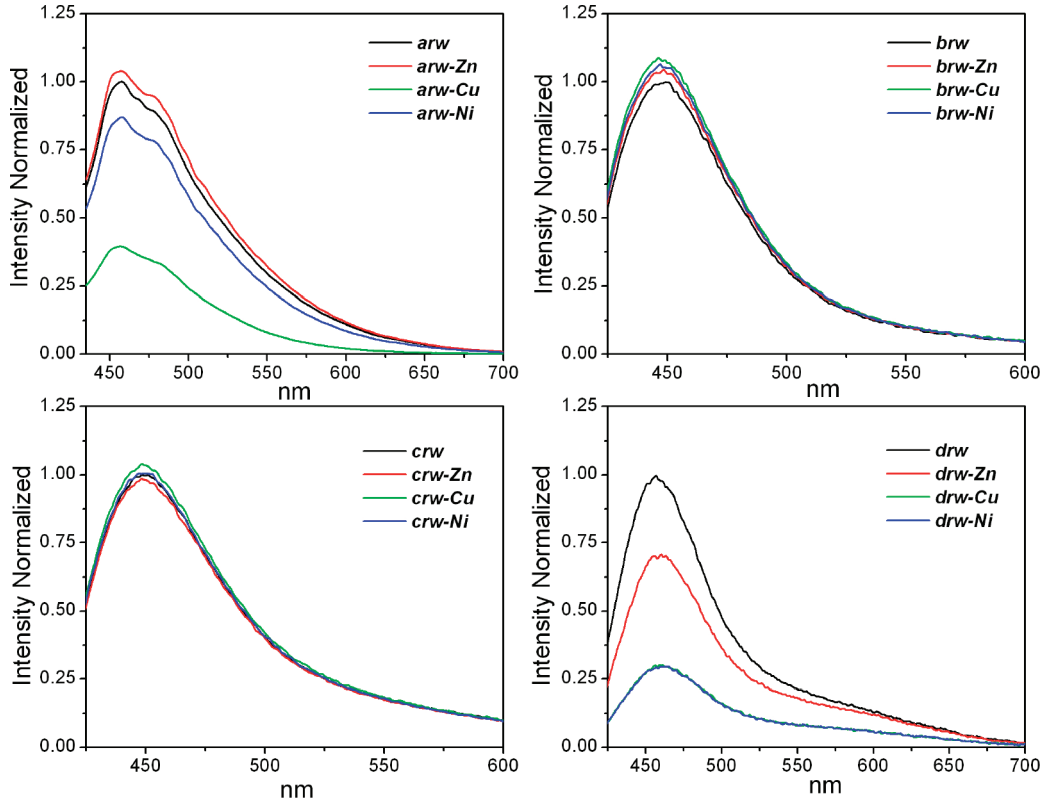

Figure 3. Fluorescence emission spectral changes of ***rw*** supported in the different resins with 0.01 M solutions of Zn^{2+}, Cu^{2+}, and Ni^{2+}, at $\lambda_{ex} = 395$ nm.

indicator. The presence of Zn^{2+} enhanced the intensity of emission, according to previous reports in other system, which contain the coordination unit EDTA.[32–34] This increase in the intensity of emission is produced when a chelating unit is coordinated to the zinc ion; the structural rigidity of the complex molecule increases the quantum efficiency of fluorescence.[33,35,36] The presence of Cu^{2+} and Ni^{2+} ions quenched the emission of fluorophore, indicating a typical behavior of paramagnetic ions. These metals have unpaired d-electrons (d^9 for Cu^{2+} and d^8 for Ni^{2+}). A paramagnetic ion reduces the forbiddingness of transitions involving a change in spin, and thus causes an increase in the rate of

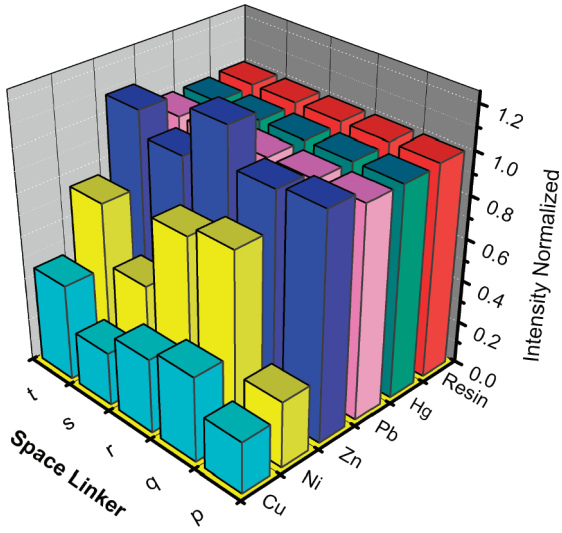

Figure 4. Normalized fluorescence response of the library using resin ***a*** and fluorescence motif ***w***, toward transition metal ions Cu^{2+}, Zn^{2+}, Ni^{2+}, Hg^{2+}, and Pb^{2+}.

intersystem crossing and a decrease in fluorescence. The electric fields associated with unpaired electrons also perturb electron spins and promote intersystem crossing.[37]

Binding and Sensing Properties toward Cu^{2+}, Zn^{2+}, and Ni^{2+}. To evaluate the binding properties of resin ***4arw*** toward Cu^{2+}, Zn^{2+}, and Ni^{2+}, the resin bead was screened for its metal ion binding capacity by the continuous flow method, according to the following methodology. A given amount of ***4arw*** resin was packed into the flow cell and a solution 5 mM of metal ion was passed continuously. The spectra were recorded every 15 s until the system becomes saturated. Sorption profiles for Cu^{2+}, Zn^{2+}, and Ni^{2+} by the ***4arw*** member library is shown in Figure 5. As expected the fluorescence intensity of ***4arw*** was quenched by Cu^{2+} and Ni^{2+}, and increased with Zn^{2+}. A continuous change in the fluorescence signal with the contact time of the metal with the resin can also be observed.

To assess if the ***4arw*** resin shows a preferential binding toward Cu^{2+} over the other cations, the same experiment was performed in the presence of Ni^{2+} and Zn^{2+} metal ions. As shown in Figure 6, the response of Cu^{2+} is not significantly different than in presence of Zn^{2+} and Ni^{2+}, indicating greater affinity for Cu^{2+} than for Zn^{2+} and Ni^{2+}. This fact also means that copper can be detected in the presence of similar concentrations of zinc. However, when the experiment was done with Zn^{2+} and Ni^{2+} together, a significant variation of the response profile was appreciated, compared to the response with the individual ions, indicating similar affinity. Thus, this study reveals that resin ***4arw*** shows selectivity and sensitivity as a dosimeter for cooper.

Sorption Characteristics and Kinetics of Reaction on Solid-Phase. The sorption of Cu^{2+} on the EDTA amide *x*-aminenaphthalene-*y*-sulfonic acid resin **4**(***a***)(***p*−*t***)(***w***) was studied, using the same methodology described above for the study of binding and sensing properties. The direct monitoring of the reaction progress on solid support was carried out by measuring the quenching of fluorescence because of the coordination reaction of copper with EDTA units. The fluorescence intensity of the beads reflected the

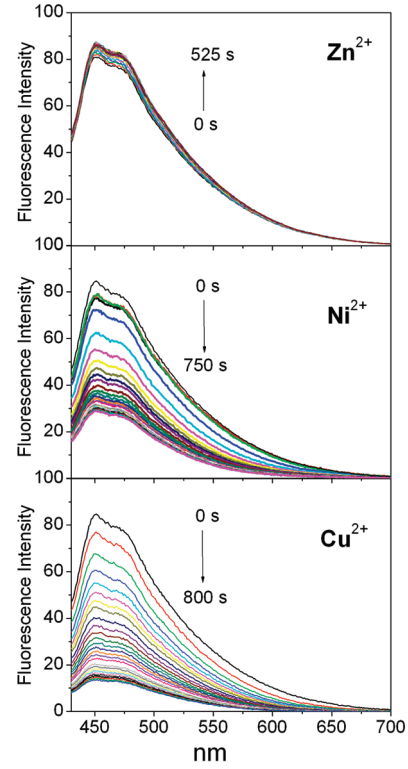

Figure 5. Sorption profiles in flow for Zn^{2+}, Ni^{2+}, and Cu^{2+} by the ***4arw*** library member. Flow rate, 1.2 mL/min; metal solutions, 5 mM.

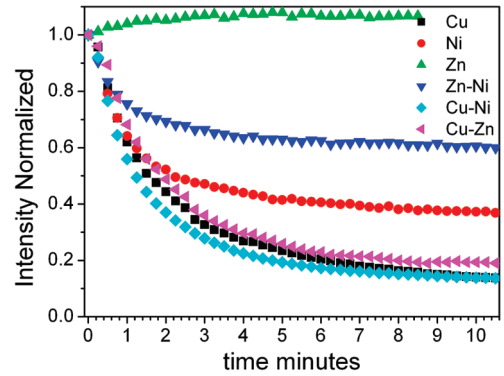

Figure 6. Dependence of the fluorescence intensity of ***4arw*** on time (λ_{ex}= 395 nm, λ_{em}= 457 nm), toward Cu^{2+}, Zn^{2+}, and Ni^{2+}, at pH 7. Flow rate, 1.2 mL/min; 5 mM metal solutions.

progression of the complexation reaction, and in this manner, real-time monitoring of the fluorescence provided valuable kinetic information. Figure 7 shows the change on fluorescence intensity of the materials studied during the time. Kinetics of the coordination reaction on the different derivative resins **4**(***a***)(***p*−*t***)(***w***) showed that the time course of the reaction fitted to second order reaction. Kinetic data are collected in Table 2. It is known that more than 99% of the reactive binding sites on the resin beads are located in the pores of the resin, and reactions at these sites are diffusion-controlled.[38] As can be seen in Table 2, the rate of reaction increases with increasing the linker length having a maximum value for hexyl derivative (***s***), indicating that it could afford restriction of diffusion, this being the rate-limiting step. For octyl derivative, the rate of reaction become smaller possibly associated with an increase of interactions

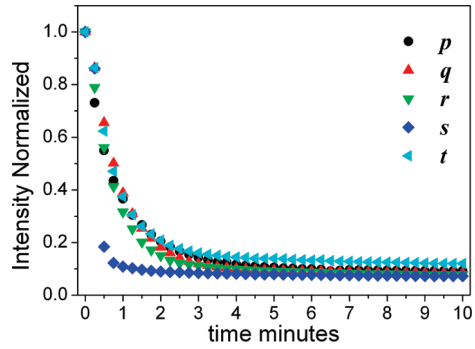

Figure 7. Time-dependent fluorescence intensity decays of materials ***4a*(*p*−*t*)*w*** in the presence of Cu^{2+} 5 mM solution. λ_{exc}= 395 nm, λ_{em}= 454 nm, flow rate 1.2 mL/min.

Table 2. Kinetic Parameters Resulting for the Sorption of Cu^{2+} on ***4a*(*p*−*t*)*w***

space linker	R^2	k^a (I^{-1} min^{-1})	$t_{1/2}$ (min^{-1})
p[b]	0.9987	2.0010	0.5799
q[b]	0.9940	2.5099	0.9214
r[b]	0.9943	3.0803	0.7881
s[b]	0.9674	9.3866	0.3511
t[b]	0.9971	1.9935	0.6682

[a] *k*= rate of reaction. [b] Second order.

Table 3. Recovery of Copper from Materials ***4a*(*p*−*t*)*w***

space linker	resin mg	Cu^{2+} mg	Cu^{2+} mg/ resin mg
p	11.25	27.32	2.43
q	14.30	54.00	3.80
r	14.10	57.20	4.05
s	10.70	52.40	4.90
t	12.85	41.30	3.24

between the fluorescent dye and the solid support, such as hydrogen bonding and other non specific interactions.

The amount of metal adsorbed by the modified resins (***a***)(***p*−*t***)(***w***) was calculated from the differences between the metal concentration before and after the contact with the resin, using the following equation:

$$Q = (C_o - C_f) \times V/M$$

where Q is the metal uptake (μg, mg^{-1}), C_o and C_f are the concentrations of Cu^{2+} before and after the contact with the resin, V is the solution volume (mL), and M is the mass of sorbent (mg). Data in Table 3 clearly demonstrate that all materials have the capacity of recovering copper, but material based in ***s*** is superior for sorption of the metal ion. They behave as a dosimeter, but the material ***4asw*** shows the best properties. It is interesting to emphasize, as was indicated previously, that the formation constant is higher in derivatives ***s*** (Table 2).

Conclusions

In conclusion, EDTA amide *x*-aminenaphthalene-*y*-sulfonic acid receptors bound to different solid supports were synthesized, and their properties as sensing phases and chelating resins toward Cu^{2+}, Zn^{2+}, Hg^{2+}, Pb^{2+}, and Ni^{2+} metal ions were evaluated. The results demonstrated that chemosensors based in an enhancement or quenching of fluorescence by charge transfer or photoinduced electron transfer, can be developed on solid phase. The study of analytical potential of library members revealed that the nature of the resin, as well as the length of the linker unit and the position of the substituent groups in the fluorophore, determine the responses of material sensing. ***4arw*** presented the best properties and showed selectivity and sensitivity as a dosimeter for cooper. The results shown establish the great potential in developing new sensing systems on solid supports.

Experimental Section

Materials. ArgoPore-Cl with 1.2 mmol/g loading was purchased from Argonaut Technologies Inc. Merrifield (98%) 4% cross-linked with DVB, Merrifield 98%, 1% linked with DVB and Wang−OH were purchased from Advanced ChemTech Inc. with 1.2, 1.1, and 0.6 mmol/g loading, respectively. EDTA-dianhydride and 5-amino-2-naphthalene sulfonic acid were purchased from Aldrich. Ethane-1,2-diamine, propane-1,3-diamine, butane-1,4-diamine, hexane-1,6-diamine, and octane-1,8-diamine were purchased from Sigma. Butane-1,4-diamine was purchased from Across Organic. 1-Naphthylamine-7-sulfonic acid, 1-naphthylamine-4-sulfonic acid, and 1-naphthylamine-5-sulfonic acid were purchased from Fluka. *N*,*N*′-Dimethylformamide and potassium carbonate were purchased from Fermont. All chemicals and solvents were of analytical reagent grade and used without further purification, except DMF, which was dried using molecular sieves. Mercury chloride, lead chloride, and nickel chloride were purchased from J. T. Baker cupric chloride from Mallinckrodt, and zinc chloride from Fermont. Working standard solutions of Cu^{2+}, Zn^{2+}, Ni^{2+}, Pb^{2+}, and Hg^{2+} (as chloride salts) at different concentration were prepared in deionized water.

Instrumentation. Infrared (IR) spectra were recorded on a Perkin-Elmer FT-IR 1600 spectrometer. Mass spectra were obtained on a Hewlett-Packard 5989 MS spectrometer at 70 eV by direct insertion. UV−vis spectra were recorded on a Perkin-Elmer Lambda 20 using diffuse reflectance. The fluorescence spectra were obtained on a Shimadzu RF-5301 PC Spectrometer. A single flow injection system equipped with a Hellma model 176.52 flow cell (25 μL) was used for assays. Measures of fluorescence intensity were obtained directly from the resin beads. All experiments were carried out at 20 ± 2 °C. Mass spectra were obtained on Agilent 1100 Series LC/MSD Trap 9.

Chlorination Method. Wang resin was chlorinated with BTC/PPh_3P, according to the chlorination method used in previous work.[27]

Chlorinated Product Wang-Cl: 1.4 g (recovery 95%), conversion 100%; IR (KBr) 3022, 2922, 1602, 1510, 1492, 1446, 1232, 1016 cm^{-1}.

General Method for the Synthesis of Alkyl Diamines on Merrifield 4% DVB, Merrifield 1% DVB, ArgoPore 5% DVB, and Wang-Cl 1%. All resins were used under the same reaction conditions to support alkyl diamines.

Portions of 1.2 g of the resins Argopore-Cl (***a***) (1.2 mmol), Merrifield 4% (***b***) (1.2 mmol), Merrifield 1% (***c***) (1.1 mmol), and Wang (***d***) (0.6 mmol) were placed in the reaction flasks and suspended in DMF (10 mL). Then K_2CO_3 (5 equiv) and alkyldiamine (5 equiv) were added, and the mixture was

allowed to react at room temperature for 24 h. Then, the resin was filtered and washed with water (3 × 20 mL), DMF (1 × 10 mL), H_2O (1 × 10 mL), methanol (3× mL), CH_2Cl_2 (1 × 10 mL), and ether (1 × 10 mL). Finally, the resins were dried under reduced pressure. Products were characterized by IR and the Kaiser Test.

***2ap*:** 1.2 g (98%), conversion 98%; IR (KBr) 3433, 3412, 3034, 2933, 1648, 1607, 1493, 1448, 1119, 1030, 897 cm^{-1}; FI = 312 au; λ_{em} = 518 nm (λ_{ex} = 467 nm).

***2aq*:** 1.2 g (96%), conversion 97%; IR (KBr) 3435, 3409, 3034, 2933, 1648, 1605, 1494, 1448, 1119, 1029, 896 cm^{-1}; FI = 308 au; λ_{em} = 526 nm (λ_{ex} = 467 nm).

***2ar*:** 1.2 g (98%), conversion 97%; IR (KBr) 3430, 3414, 3034, 2933, 1647, 1606, 1491, 1446, 1120, 1029, 896 cm^{-1}; FI = 288 au; λ_{em} = 526 nm (λ_{ex} = 467 nm).

***2as*:** 1.2 g (99%), conversion 98%; IR (KBr) 3422, 3371, 3034, 2933, 1648, 1607, 1493, 1448, 1119, 1030, 897 cm^{-1}; FI = 359 au; λ_{em} = 527 nm (λ_{ex} = 467 nm).

***2at*:** 1.2 g (96%), conversion 97%; IR (KBr) 3429, 3409, 3034, 2933, 1646, 1607, 1493, 1448, 1120, 1029, 899 cm^{-1}; FI = 308 au; λ_{em} = 526 nm (λ_{ex} = 467 nm).

***2bp*:** 1.2 g (96%), conversion 98%; IR (KBr) 3369, 3082, 3060, 3026, 2915, 2857, 1597, 1492, 1449, 1368, 1267, 1110, 902, 819 cm^{-1}. FI = 363 au; λ_{em} = 454 nm (λ_{ex} = 373 nm).

***2br*:** 1.2 g (96%), conversion 98%; IR (KBr) 3361, 3081, 3060, 3026, 2915, 2857, 1597, 1492, 1450, 1368, 1267, 1113, 903, 819 cm^{-1}; FI = 287 au; λ_{em} = 454 nm (λ_{ex} = 377 nm).

***2bs*:** 1.2 g (96%), conversion 98%; IR (KBr) 3408, 3081, 3060, 3028, 2915, 2857, 1597, 1492, 1449, 1366, 1267, 1112, 904, 819 cm^{-1}; FI = 196 au; λ_{em} = 451 nm (λ_{ex} = 368 nm).

***2cp*:** 1.2 g (95%), conversion 96%; IR (KBr) 3414, 3057, 2928, 1663, 1601, 1492, 1450, 1372, 1182, 1024, 907, 816 cm^{-1}; FI = 224 au; λ_{em} = 444 nm (λ_{ex} = 366 nm).

***2cq*:** 1.2 g (95%), conversion 97%; IR (KBr) 3415, 3024, 2926, 1663, 1601, 1491, 1449, 1372, 1182, 1023, 906, 818 cm^{-1}; FI = 286 au; λ_{em} = 448 nm (λ_{ex} = 359 nm).

***2ct*:** 1.2 g (95%), conversion 96%; IR (KBr) 3297, 3024, 2921, 1671, 1600, 1492, 1450, 1371, 1182, 1028, 906, 819 cm^{-1}; FI = 290 au; λ_{em} = 450 nm (λ_{ex} = 378 nm).

***2dp*:** 1.2 g (97%), conversion 98%; IR (KBr): 3297, 3024, 2921, 1671, 1600, 1492, 1450, 1371, 1182, 1028, 906, 819 cm^{-1}; FI = 257 au; λ_{em} = 441 nm (λ_{ex} = 372 nm).

***2dr*:** 1.2 g (98%), conversion 97%; IR (KBr) 3297, 3024, 2921, 1671, 1600, 1492, 1450, 1371, 1182, 1028, 906, 819 cm^{-1}; FI = 207 au; λ_{em} = 440 nm (λ_{ex} = 374 nm).

***2ds*:** 1.2 g (95%), conversion 97%; IR (KBr) 3297, 3024, 2921, 1671, 1600, 1492, 1450, 1371, 1182, 1028, 906, 819 cm^{-1}; FI = 199 au; λ_{em} = 445 nm (λ_{ex} = 371 nm).

General Method for the Synthesis of EDTA Dianhydride and Derivatives of Amino Naphthalesulfonic Acid Supported on Merrifield's, Argopore, and Wang Modified with Alkyldiamines. In separate reaction vessels, ***a*−(*p*−*t*)** (200 mg, 1.2 mmol, 1 NH_2), ***b*−(*p*−*t*)** (200 mg, 1.2 mmol, 1 NH_2), ***c*−(*p*−*t*)** (200 mg, 1.1 mmol, 1 NH_2), and ***d*−(*p*−*t*)** (200 mg, 0.6 mmol, 1 NH_2) were suspended in dry DMF (10 mL), and then 3 equiv of EDTA dianhydride was added. The vessels were stirred for 24 h and then added 5 equiv of derivatives of ANS (1-naphthylamine-4-sulfonic acid (***w***), 1-naphthylamine-5-sulfonic acid(***x***), 1-naphthylamine-7-sulfonic acid (***y***), or 5-naphthylamine-2-sulfonic acid (***z***)), and the mixtures were stirred for 24 h. The suspension was filtered and washed with a saturated solution of Na_2CO_3 (4 × 30 mL), H_2O (2 × 30 mL), CH_3OH (2 × 20 mL), CH_2Cl_2 (2 × 10 mL), and ether (2 × 10 mL). Finally, the resin was dried under reduced pressure.

For the mass spectrometry analysis, the resins were treated with TFA/CH_2Cl_2 (1:1) for 30 min.

***4apw*:** 0.2 g (99%), conversion 98%; IR (KBr) 3319, 1723, 1671, 1631, 1592, 1493, 1448, 1410, 1220, 1113, 1049, 761, 540 cm^{-1}; FI = 176 au; λ_{em} = 456 nm (λ_{ex} = 397 nm).

4apx: 0.2 g (98%). conversion 97%; IR (KBr) 3420, 3282, 3022, 1746, 1670, 1629, 1591, 1489, 1455, 1407, 1223, 1119, 1049, 761, 571 cm^{-1}; FI = 13 au; λ_{em} = 477 nm (λ_{ex} = 396 nm).

***4aqw*:** 0.2 g (97%) conversion 97%; IR (KBr) 3324, 1725, 1670, 1632, 1593, 1493, 1450, 1410, 1221, 1113, 1050, 761, 541 cm^{-1}; FI = 174 au; λ_{em} = 456 nm (λ_{ex} = 396 nm); ESI-MS (*m*/*z*) 554.3$[L + H]^+$.

***4arw*:** 0.2 g (98%), conversion 98%; IR (KBr) 3314, 1727, 1673, 1629, 1594, 1493, 1448, 1410, 1220, 1116, 1049, 761, 539 cm^{-1}, FI = 177 au; λ_{em} = 458 nm (λ_{ex} = 398 nm); ESI-MS (*m*/*z*) 567.3 $[L + H]^+$.

***4arz*:** 0.2 g (97%), conversion 98%; IR (KBr) 3314, 1728, 1667, 1629, 1594, 1493, 1448, 1410, 1220, 1116, 1033, 761, 545 cm^{-1}; FI = 32 au; λ_{em} = 458 nm (λ_{ex} = 395 nm); ESI-MS (*m*/*z*) 567.3$[L + H]^+$.

4asw: 0.2 g (96%), conversion 98%; IR (KBr) 3318, 1725, 1670, 1630, 1594, 1493, 1448, 1410, 1219, 1114, 1049, 761, 540 cm^{-1}; FI = 158 au; λ_{em} = 457 nm (λ_{ex} = 395 nm); ESI-MS (*m*/*z*) 595.2 $[L + H]^+$.

4atw: 0.2 g (96%), conversion 97%; IR (KBr) 3320, 1724, 1675, 1630, 1595, 1493, 1448, 1410, 1222, 1118, 1049, 761, 537 cm^{-1}; FI = 54 au; λ_{em} = 461 nm (λ_{ex} = 395 nm); ESI-MS (*m*/*z*) 623.3 $[L + H]^+$.

4bpx: 0.2 g (97%), conversion 98%; IR (KBr) 1724, 1677, 1626, 1595, 1569, 1481, 1402, 1314, 1278, 1198, 1050, 960, 522 cm^{-1}; FI = 212 au; λ_{em} = 441 nm (λ_{ex} = 390 nm).

***4bqz*:** 0.2 g (96%), conversion 97%; IR (KBr) 1723, 1674, 1626, 1595, 1569, 1481, 1402, 1314, 1268, 1197, 1048, 960, 527 cm^{-1}; FI = 24 au; λ_{em} = 443 nm (λ_{ex} = 396 nm).

4brw: 0.2 g (97%), conversion 98%; IR (KBr) 3228, 3014, 1745, 1719, 1659, 1622, 1564, 1544, 1439, 1422, 1318, 1260, 1185, 1065, 903, 522 cm^{-1}; FI = 125 au; λ_{em} = 448 nm (λ_{ex} = 397 nm); ESI-MS (*m*/*z*) 567.4 $[L + H]^+$.

4bsz: 0.2 g (96%), conversion 96%; IR (KBr) 1739, 1720, 1675, 1632, 1599, 1489, 1449, 1383, 1320, 1276, 1168, 1041, 906, 536 cm^{-1}; FI = 124 au; λ_{em} = 435 nm (λ_{ex} = 396 nm).

4bty: 0.2 g (96%), conversion 97%; IR (KBr) 3256, 1732, 1691, 1632, 1548, 1411, 1277, 1201, 1170, 1041, 1097, 898, 507 cm^{-1}; FI = 35 au; λ_{em} = 435 nm (λ_{ex} = 394 nm).

4cpy: 0.2 g (97%), conversion 98%; IR (KBr) 1731, 1682, 1632, 1600, 1574, 1532, 1413, 1275, 1200, 1112, 963, 757, 500 cm^{-1}; FI = 3 au; λ_{em}= 451 nm (λ_{ex} = 390 nm).

4cqx: 0.2 g (96%), conversion 98%; IR (KBr) 1729, 1681, 1597, 1487, 1409, 1205, 1112, 943, 908, 758, 531 cm^{-1}; FI = 48 au; λ_{em} = 433 nm (λ_{ex} = 396 nm).

4crw: 0.2 g (97%), conversion 97%; IR (KBr) 1729, 1676, 1601, 1487, 1449, 1275, 1191, 1122, 1049, 955, 907, 756, 526 cm^{-1}; FI = 45 au; λ_{em} = 446 nm (λ_{ex} = 398 nm).

4csz: 0.2 g (97%), conversion 96%; IR (KBr) 1732, 1669, 1698, 1484, 1450, 1273, 1181, 1120, 1049, 955, 906, 755, 528 cm^{-1}; FI = 6 au; λ_{em}= 453 nm (λ_{ex} = 397 nm).

4ctw: 0.2 g (96%), conversion 97%; IR (KBr) 1732, 1672, 1600, 1486, 1450, 1273, 1181, 1123, 1050, 955, 907, 755, 526 cm^{-1}; FI = 28 au; λ_{em}= 450 nm (λ_{ex} = 396 nm).

4dpw: 0.2 g (95%), conversion 97%; IR (KBr) 3401, 1739, 1683, 1627, 1562, 1440, 1369, 1236, 1192, 1111, 1024, 748, 530 cm^{-1}; FI = 12 au; λ_{em}= 451 nm (λ_{ex} = 397 nm).

4dqx: 0.2 g (96%), conversion 97%; IR (KBr) 3421, 1741, 1682, 1627, 1562, 1440, 1369, 1236, 1192, 1121, 1024, 748, 532 cm^{-1}; FI = 9 au; λ_{em}= 435 nm (λ_{ex} = 394 nm).

4drw: 0.2 g (96%), conversion 97%; IR (KBr) 3418, 1740, 1682, 1627, 1562, 1440, 1369, 1236, 1192, 1118, 1024, 748, 535 cm^{-1}; FI = 66 au; λ_{em} = 454 nm (λ_{ex} = 395 nm); ESI-MS (*m*/*z*) 567 $[L + H]^+$.

4dry: 0.2 g (95%), conversion 97%; IR (KBr) 3433, 1742, 1682, 1627, 1562, 1440, 1369, 1236, 1192, 1127, 1024, 748, 533 cm^{-1}; FI = 24 au; λ_{em} = 445 nm (λ_{ex} = 396 nm); ESI-MS (*m*/*z*) 567.2 $[L + H]^+$.

4dsz: 0.2 g (97%), conversion 98%; IR (KBr) 3433, 1740, 1682, 1627, 1562, 1440, 1369, 1236, 1192, 1124, 1024, 748, 535 cm^{-1}; FI = 56 au; λ_{em} = 454 nm (λ_{ex} = 396 nm).

4dtw: 0.2 g (96%), conversion 97%; IR (KBr) 3428, 1739, 1682, 1627, 1562, 1440, 1369, 1236, 1192, 1128, 1024, 748, 534 cm^{-1}; FI = 35 au; λ_{em} = 449 nm (λ_{ex} = 397 nm).

Acknowledgment. We gratefully acknowledge the support for this project by Consejo Nacional de Ciencia y Tecnología, Mexico (CONACyT, Grant No SEP-CO1-47835-U) and Direccion General de Educaion Superior Tecnologica (DGEST-2008). H.S. thanks CONACyT and University of Sonora for a postdoctoral fellowship.

Supporting Information Available. Additonal experimental details, table of absorption and fluorescence data, and figures showing fluorescence intensity and emission spectra. This material is available free of charge via the Internet at http://pubs.acs.org.

References and Notes

(1) Alarcon, J.; Aucejo, R.; Albelda, M. T.; Alves, S.; Clares, M. P.; Garcia-España, E.; Lodeiro, C.; Marchin, K. L.; Parola, A. J.; Pina, F.; Seixas de Melo, J.; Soriano, C. *Supramol. Chem.* **2004**, *16*, 573–580.
(2) Alves, S.; Pina, F.; Albelda, M. T.; Garcia-España, E.; Soriano, C.; Luis, S. V. *Eur. J. Inorg. Chem.* **2001**, 405–412.
(3) Kim, K. S.; Jun, E. J.; Kim, S.; Choi, H. J.; Yoo, J.; Lee, C. H.; Hyun, M. H.; Yoon, J. *Tetrahedron Lett.* **2007**, *48*, 2481–2484.
(4) Chang, J. H.; Choi, Y. M.; Shin, Y. L. *Bull. Korean Chem. Soc.* **2001**, *22*, 527–530.
(5) Kwon, J. Y.; Soh, J. H.; Yoon, Y. J.; Yoon, J. *Supramol. Chem.* **2004**, *16*, 621–624.
(6) Yoon, Y. *J. Ind. Eng. Chem.* **1999**, *5*, 212–217.
(7) Bargossi, C.; Fiorini, M. C.; Montalti, M.; Prodi, L.; Zaccheroni, N. *Coord. Chem. Rev.* **2000**, *208*, 17–32.
(8) Kantipuly, C.; Katragadda, S.; Chow, A.; Gesser, H. D. *Talanta* **1990**, *37*, 491–517.
(9) Yang, J.; Renken, A. *Chem. Eng. Technol.* **2000**, *23*, 1007–1012.
(10) Sharaf, M. A.; Sayed, S. A.; Younis, A. A.; Farag, A. B.; Arida, H. A. *Anal. Lett.* **2007**, *40*, 3443–3456.
(11) Prabhakaran, D.; Subramanian, M. S. *React. Funt. Polym.* **2003**, *57*, 147–155.
(12) Ji, C. N.; Qu, R. J.; Wang, C. H.; Sun, C. M.; Tang, Q. H. *Chin. Chem. Lett.* **2005**, *16*, 1193–1196.
(13) Lee, W.; Lee, S. E.; Kim, M. K.; Lee, C. H.; Kim, Y. S. *Bull. Korean Chem. Soc.* **2002**, *23*, 1067–1072.
(14) Jyo, A.; Hiwatashi, I.; Weber, R.; Egawa, H. *Anal. Sci.* **1992**, *8*, 195–200.
(15) Yang, J.; Renken, A. *Chem. Eng. Technol.* **2000**, *23*, 1007–1012.
(16) Prabhakaran, D.; Subramanian, M. S. *Talanta* **2003**, *61*, 431–437.
(17) Terada, K. *Anal. Sci.* **1991**, *7*, 187–198.
(18) Garg, B. S.; Sharma, R. K.; Bhojak, N.; Mittal, S. *Microchem. J.* **1999**, *61*, 94–114.
(19) Türker, A. R. *Clean: Soil, Air, Water* **2007**, *35*, 548–557.
(20) Ebraheem, K. A. K.; Hamdi, S. T. *React. Funt. Polym.* **1997**, *34*, 5–10.
(21) Wang, C. C.; Wang, C. C. *J. Appl. Polym. Sci.* **2005**, *97*, 2457–2468.
(22) Bicak, N.; Senkal, B. F.; Melekaslan, D. *J. Appl. Polym. Sci.* **2000**, *77*, 2749–2755.
(23) Clausen, A. M.; Carr, P. W. *Anal. Chem.* **1998**, *70*, 378–385.
(24) Varma, A. J.; Deshpande, S. V.; Kennedy, J. F. *Carbohydr. Polym.* **2004**, *55*, 77–93.
(25) Geckeler, K. E. *Pure Appl. Chem.* **2001**, *73*, 129–136.
(26) Rivero, I. A.; Somanathan, R.; Hellberg, L. H. *Synth. Commun.* **1993**, *23*, 711.
(27) Rivero, I. A.; Gonzalez, T.; Pina-Luis, G.; Diaz-Garcia, M. E. *J. Comb. Chem.* **2005**, *7*, 46–53.
(28) Wiczk, W.; Rzeska, A.; Łukanska, J.; Stachowiak, K.; Karulczak, J.; Malicka, J.; Łankiewicz, L. *Chem. Phys. Lett.* **2001**, *341*, 99–106.
(29) Chernilevskaya, G. S.; Aksiment'va, E. I.; Novikov, V. P. *Theor. Experim. Chem.* **1997**, *33*, 21–25.
(30) Vaino, A. R.; Janda, K. D. *J. Comb. Chem.* **2000**, *2*, 579–596.
(31) Silva, E. H.; Etchegaray, A.; Carvalho, R. S. H.; Jubilut, G. N.; Miranda, A.; Nakaie, C. R. *J. Braz. Chem. Soc.* **2005**, *16*, 171–178.
(32) Inoue, M. B.; Muñoz, I. C.; Inoue, M.; Fernando, Q. *Inorg. Chim. Acta* **2000**, *300*−*302*, 206–211.
(33) Machi, L.; Santacruz, H.; Sanchez, M.; Inoue, M. *Supramol. Chem.* **2006**, *7*, 561–569.
(34) Machi, L.; Santacruz, H.; Sanchez, M.; Inoue, M. *Inorg. Chem. Commun.* **2007**, *10*, 547–550.
(35) Rurak, K. *Spectrochim. Acta A.* **2001**, *57*, 2161–2195.
(36) Be'reau, V. *Inorg. Chem. Commun.* **2004**, *7*, 829–833.
(37) Seitz, W. R.; Frei, R. W. *Crit. Rev. Anal. Chem.* **1980**, *8*, 367–405.
(38) Pina-Luis, G.; Badìa, R.; Diaz-Garcia, M. E.; Rivero, I. A. *J. Comb. Chem.* **2004**, *6*, 391–397.

CC900075R